Design and Development of Novel 2-D Oligomers for Electroactive Device Application†

Zukhra I. Niazimbetova,§ Hermona Y. Christian,§ Yashpal J. Bhandari,§ Frederick L. Beyer,‡ and Mary E. Galvin*,§

Department of Materials Science and Engineering, University of Delaware, Newark, Delaware 19716, and U.S. Army Research Laboratory, Polymer Research Branch, Building 4600, Aberdeen Proving Ground, Maryland 21005

Received: October 14, 2003; In Final Form: March 16, 2004

Four novel two-dimensional conjugated poly(*p*-phenylenevinylene) (PPV)-based molecules have been synthesized, characterized, and evaluated for use in light-emitting diodes (LEDs). These novel molecules all contain a tetra-substituted central phenyl ring, but the length, chemical structure, and placement of the arms is varied in order to tailor their hole and electron transport properties. The materials are all solution-processible, maintain conjugation through the arms and central core, and exhibit evidence of two- and possibly three-dimensional charge delocalization. The first molecule contains four phenylenevinylene arms with solubilizing octyloxy-substituted units. Two of the molecules have two phenylenevinylene arms and two oxadiazole arms that are placed ortho or para with respect to each other. The fourth molecule contains four cyano-phenylenevinylene arms with solubilizing octyloxy groups at the ends of each arm. As a class these molecules all have large Stokes shifts in films, although the propensity for $\pi-\pi$ stacking varies between the molecules. The oxadiazole-containing molecules show promise for applications in single-layer LEDs.

Introduction

In recent years, the development of conjugated organic and polymeric materials has seen great progress due to their potential applications in optoelectronic devices, such as light-emitting diodes (LEDs), photovoltaics (PVs), and thin film transistors (TFTs).[1−4] While these materials possess electronic properties similar to inorganic semiconductors, they also provide the added advantages of low cost, ease of fabrication, and mechanical flexibility. Despite these desirable features, a serious limitation in these materials is poor charge transport.[5] Polymers typically transport charges in one dimension, along the conjugated backbone. Three-dimensional transport is achieved and limited by the inefficient and slow process of interchain hopping. Charge mobility, and hence device efficiency, can be improved if charges are more easily delocalized across two and even three dimensions.

In linear conjugated polymers, two-dimensional transport can be achieved by $\pi-\pi$ stacking.[6,7] This, however, increases their propensity to crystallize and favors excimer formation leading to a low photoluminescence quantum yield in films.[8] For this reason, while crystallinity may improve charge transport and thus be useful for PV and TFT applications, it is detrimental to LED performance.[9] Various groups have been working on developing materials that could intrinsically possess two-dimensional transport.[10−12] Some charge delocalization has been observed in dendrimeric molecules, although conjugation in these materials is interrupted through the metalinkages and twisting due to steric crowding around the core.[10] Robinson et al. have synthesized soluble, amorphous two-dimensional oligomers for use in optoelectronic applications.[11] These materials exhibit some properties of small molecules, such as defined molecular structure and high purity, but, like many polymers, are resistant to crystallization and are able to form homogeneous films making them useful in LEDs. These molecules, however, show only one-dimensional conjugation, since conjugation is not maintained through the core. Schmidt-Mende et al. have reported on the synthesis of a solution-processible, three-dimensionally ordered crystalline organic molecule and its use as a semiconducting material in PVs.[12] This molecule maintains charge delocalization across the phenyl rings and through $\pi-\pi$ stacking, as does graphite, but the ability to engineer the energy difference between the highest occupied molecular orbital (HOMO) and the lowest unoccupied molecular orbital (LUMO) in this material is limited.

In this paper, we report on the synthesis and potential application of four novel two-dimensional conjugated poly(*p*-phenylenevinylene) (PPV)-based oligomers for optoelectronic devices, shown in Chart 1. On the basis of prior work, it was determined that a tetra-substituted oligomer exhibited a higher quantum yield than an analogous meta-substituted species and showed promise for increased charge carrier mobility.[13] The materials described in this work are tetra-substituted, solution-processible, maintain conjugation through the arms and central core, and exhibit evidence of two- and possibly three-dimensional charge delocalization. Oligomer PPV-X, with the X denoting the shape of the molecule, is a PPV-based molecule with solubilizing octyloxy-substituted units. Since prior research has shown that oxadiazole moieties improve electron transport, LED efficiency, and photoluminescence stability,[14] an electron-deficient oxadiazole species is introduced into the PPV backbone of two para arms in oligomer *p*-OXA-X. In the ortho-substituted oligomer, *o*-OXA-X, the position of the oxadiazole species is changed in an attempt to tune the thermal and photophysical properties and to investigate the role of symmetry in determining the properties of these materials. For example, we anticipate

† Part of the special issue "Alvin L. Kwiram Festschrift".

* To whom correspondence should be addressed. E-mail: megalvin@udel.edu. Fax: (302) 831-4545. Phone: (302) 831-0873.

§ University of Delaware.

‡ U. S. Army Research Laboratory.

10.1021/jp0371074 CCC: $27.50
Published on Web 05/05/2004

CHART 1: Structure of Oligomers

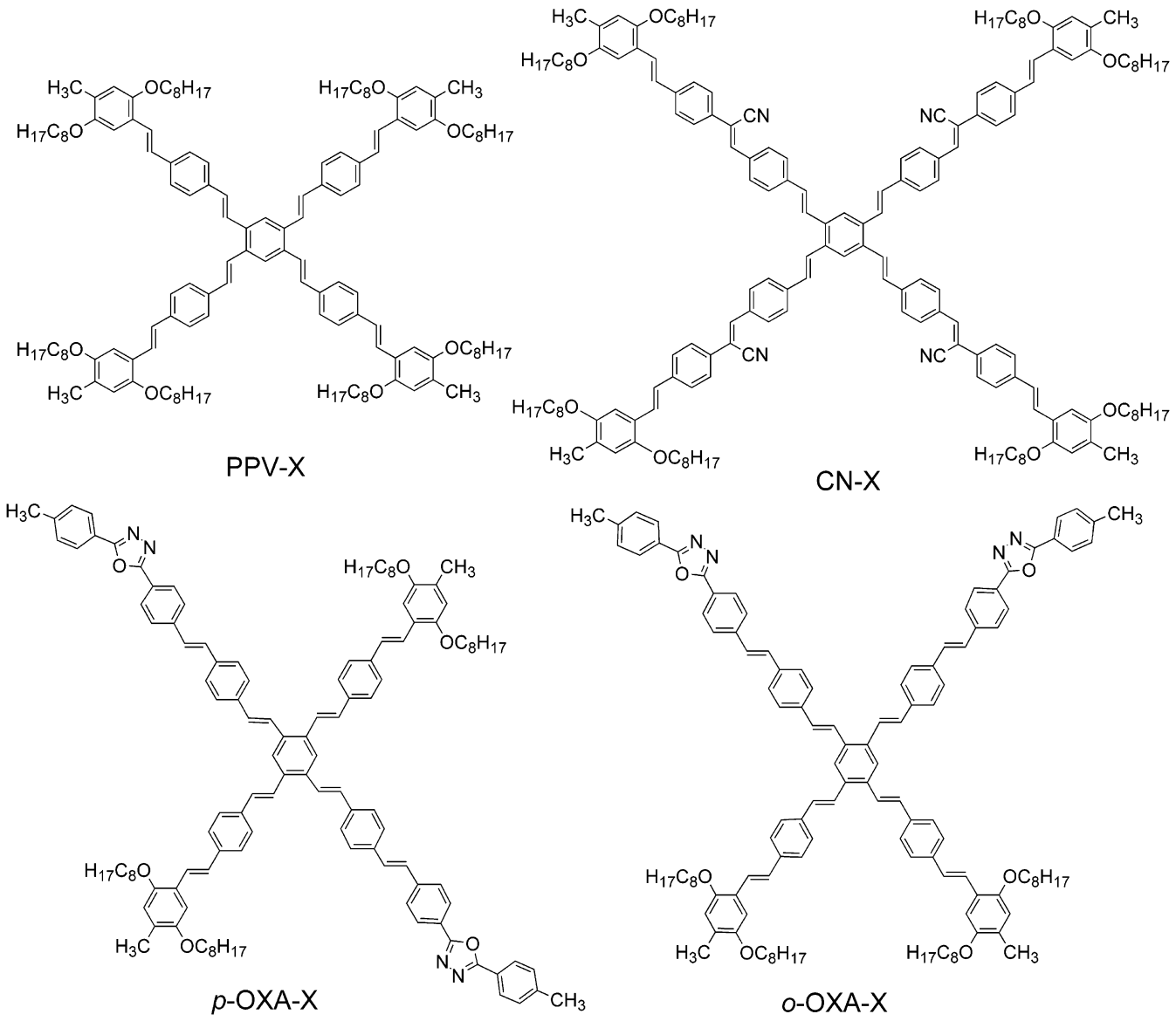

changes in the molecular packing and seek to study its effect in LED and PV performance. Finally in oligomer CN-X, an electron-transporting cyano species is introduced to improve electron transport and shift the absorption toward the red to better match the solar spectrum for PV applications.[15] Collectively these four compounds point to the synthetic flexibility of this class of molecules. Since it is possible to vary the composition and placement of each arm, it should be possible to engineer packing and HOMO/LUMO energy levels. This paper is thus a first report on this novel type of electroactive molecules, which for convenience we refer to as Xs, and their potential as the electroactive layer in applications such as LEDs and PVs.

Experimental Section

Synthesis/Characterization. All starting materials were obtained from Aldrich and used as received. Tetrakis(triphenylphosphine)palladium(0) was obtained from Lancaster; tributylvinyltin was obtained from Organometallics, Inc. Tetrahydrofuran (THF) and ethylene glycol dimethyl ether (DME) were distilled over sodium/benzophenone under nitrogen before use. 1,1,2,2-Tetrachloroethane (TCE) was purified by distillation. The syntheses of 4-vinylbenzaldehyde, 2,5-bis(diethylphosphonatomethyl)-1,4-dibromobenzene (**4**), and 4-((*E*)-2-{2,4,5-tris-[(*E*)-2-(4-formylphenyl)ethenyl]phenyl}ethenyl)benzen carbaldehyde (**8**), have been previously described.[13] Diethyl 4,5-dibromo-2-[(diethoxyphosphoryl) methyl]benzylphosphonate[16,17] (**6**), 2-(4-vinylphenyl) acetonitrile,[18] and 1,4-divinylbenzene[19] were synthesized according to literature procedures. All reactions were carried out under a dry nitrogen atmosphere using standard vacuum line techniques. Selecto Scientific and Merck silica gel (60 Å; 70−230 mesh) was used for column chromatography. Nuclear magnetic resonance (NMR) spectra were obtained with Brüker 250, 360, and 400 MHz spectrometers. IR spectra were recorded using KBr pellets on a Thermo Nicolet Nexus 670 FT-IR spectrometer. Mass spectra (MS) were obtained on a Brüker BIFLEX III (MALDI source) and a ZAB2SE (Micromass) spectrometer. Melting points were obtained with the IA9300 electrothermal digital melting point apparatus and are uncorrected. The progress of the reactions was monitored by means of thin-layer chromatography. For the synthesis of compounds **1**−**3**, **5**, **7**, and **9** see the Supporting Information.

1,2,4,5-Tetrakis[2-[4-[2-[2,5-bis(octyloxy)-4-methylphenyl] ethenyl]phenyl]ethenyl]benzene, (all-*E*), PPV-X. To a

solution of **5** (0.757 g, 0.64 mmol), tri-*o*-tolylphosphine (79 mg, 0.26 mmol), and **2** (0.763 g, 1.6 mmol) in 20 mL of dry DMF, tributylamine (0.305 mL, 1.28 mmol) was added. The mixture was heated and $Pd(OAc)_2$ (12 mg, 0.053 mmol) was then added. The resulting mixture was stirred at ~95 °C overnight under a nitrogen atmosphere. After having been cooled to room temperature, the mixture was poured into ~80 mL of methanol and the precipitate was filtered off. The crude product was purified by column chromatography using chloroform−hexane mixture as an eluent to yield PPV-X in 77% yield (0.98 g). ^{1}H NMR (400 MHz, $CDCl_3$), δ (ppm): 0.88 (t, J = 7.0 Hz, 12H, 4 × CH_3); 0.90 (t, J = 6.8 Hz, 12H, 4 × CH_3); 1.36−1.55 (m, 80H, 40 × CH_2); 1.78−1.88 (m, 16H, 8 × C*H*$_2$CH$_2$O); 2.24 (s, 12H, 4 × CH_3); 3.98 (t, J = 6.5 Hz, 8H, 4 × CH_2O); 3.99 (t, J = 6.5 Hz, 8H, 4 × CH_2O); 6.74 (s, 4H, arom); 7.06 (s, 4H, arom); 7.09 (d, J = 16.0 Hz, 4H, H_{vinyl}); 7.13 (d, J = 16.4 Hz, 4H, H_{vinyl}); 7.51 (d, J = 16.4 Hz, 4H, H_{vinyl}); 7.52 (d, J = 16.0 Hz, 4H, H_{vinyl}); 7.56 (dd, J_1 = 8.6 Hz, J_2 = 8.4 Hz, 16H, arom); 7.85 (s, 2H, arom). IR (cm^{-1}): 3057 (w), 3045 (w), 3022 (w), 2952 (s), 2922 (s), 2869 (s), 2851 (s), 2730 (w), 1625 (w), 1595 (w), 1575 (w), 1514 (s), 1503 (s), 1467 (s), 1455 (s), 1412 (s), 1383 (s), 1333 (m), 1311 (m), 1290 (m), 1275 (m), 1252 (m), 1204 (s), 1117 (m), 1047 (s), 1025 (s), 956 (s), 852 (s), 801 (s), 747 (w), 723 (m), 694 (w), 650 (w), 534 (s), 473 (w). MS (MALDI): *m*/*z* 1975.63 (M$^+$, 55% (calcd: 1975.45)); 1976.61 (^{13}C isotope peak (calcd: 1976.45) along with M + H$^+$, 69%); 1977.68 (56%), 1978.63 (33%).

2-[4-((*E*)-2-4-[(*E*)-2-(2,5-Bis[(*E*)-2-(4-(*E*)-2-[4-methyl-2,5-bis(octyloxy)phenyl]ethenylphenyl) ethenyl]-4-(*E*)-2-[4-((*E*)-2-4-[5-(4-methylphenyl)-1,3,4-oxadiazol-2-yl]phenylethenyl)-phenyl] ethenylphenyl)ethenyl]phenylethenyl)phenyl]-5-(4-methylphenyl)-1,3,4-oxadiazole, *p*-OXA-X. This compound was prepared from compound **5** (0.473 g, 0.4 mmol) and compound **3** (0.364 g, 1.0 mmol) by the same general procedure as the one used for the synthesis of PPV-X. The reaction mixture was stirred at 70 °C for 24 h. After cooling to room temperature, the mixture was poured into methanol. The yellow precipitate was collected by filtration. The product was further purified by redissolving in chloroform and filtering through a 0.45 μm syringe filter. By adding methanol the product was precipitated, collected by filtration, and then dried to give 0.602 g of *p*-OXA-X (86% yield). ^{1}H NMR (360 MHz, $CDCl_3$), δ (ppm): 0.89 (t, J = 6.5 Hz, 6H, 2 × CH_3); 0.90 (t, J = 6.1 Hz, 6H, 2 × CH_3); 1.24−1.52 (m, 40H, 20 × CH_2); 1.78−1.85 (m, 8H, 4 × C*H*$_2$CH$_2$O); 2.23 (s, 6H, 2 × CH_3); 2.43 (s, 6H, 2 × CH_3); 3.96 (t, J = 6.5 Hz, 8H, 4 × CH_2O); 6.72 (s, 2H, arom); 7.00 (d, J = 15.8 Hz, 2H, H_{vinyl}); 7.02 (d, J = 16.2 Hz, 2H, H_{vinyl}); 7.04 (s, 2H, arom); 7.05 (d, J = 16.2 Hz, 2H, H_{vinyl}); 7.08 (d, J = 16.2 Hz, 2H, H_{vinyl}); 7.14 (d, J = 16.2 Hz, 2H, H_{vinyl}); 7.30 (d, J = 8.1 Hz, 4H, arom); 7.39 (d, J = 16.2 Hz, 2H, H_{vinyl}); 7.41 (d, 15.8 Hz, 2H, arom); 7.48 (d, J = 16.2 Hz, 2H, H_{vinyl}); 7.49 (s, 8H, arom); 7.54 (s, 8H, arom); 7.56 (d, J = 8.3 Hz, 4H, arom); 7.73 (s, 2H, arom (core)); 7.98 (d, J = 8.1 Hz, 4H, arom); 8.04 (d, J = 8.3 Hz, 4H, arom). IR (cm^{-1}): 3025 (m), 2949 (s), 2923 (s), 2868 (s), 2853 (s), 1902 (w), 1801 (w), 1608 (s), 1595 (s), 1575 (m), 1554 (m), 1512 (s), 1494 (s), 1468 (s), 1456 (m), 1411 (s), 1389 (m), 1378 (m), 1334 (m), 1311 (m), 1289 (w), 1272 (m), 1247 (w), 1205 (s), 1181 (s), 1118 (w), 1100 (w), 1066 (s), 1043 (m), 1016 (s), 959 (s), 902 (w), 853 (s), 826 (s), 801 (s), 742 (m), 728 (s), 701 (m), 544 (s), 532 (m), 500 (w), 475 (w). MS (MALDI, dithranol (1,8-dihydroxy-9(10*H*)anthracenone) was used as a matrix with silver trifluoroacetate to enhance cationization): *m*/*z* 1857.69 (M$^+$ + ^{107}Ag$^+$); 1859.71 (M$^+$ + ^{109}Ag$^+$).

2-[4-((*E*)-2-4-[(*E*)-2-(4,5-Bis[(*E*)-2-(4-(*E*)-2-[4-methyl-2,5-bis(octyloxy)phenyl]ethenylphenyl) ethenyl]-2-(*E*)-2-[4-((*E*)-2-4-[5-(4-methylphenyl)-1,3,4-oxadiazol-2-yl]phenylethenyl)-phenyl] ethenylphenyl)ethenyl]phenylethenyl)phenyl]-5-(4-methylphenyl)-1,3,4-oxadiazole, *o*-OXA-X. This compound was prepared from compound **7** (300.8 mg, 0.254 mmol) and **3** (434.5 mg, 1.193 mmol) by the procedure described above for the synthesis of PPV-X. The crude product was purified by column chromatography first using a chloroform−hexane mixture then THF as an eluent to yield *o*-OXA-X (yellow solid) in 67% yield (0.334 g). ^{1}H NMR (360 MHz, $CDCl_3$), δ (ppm): 0.88 (t, J = 6.8 Hz, 6H, 2 × CH_3); 0.90 (t, J = 6.2 Hz, 6H, 2 × CH_3); 1.26−1.58 (m, 40H, 20 × CH_2); 1.78−1.88 (m, 8H, 4 × C*H*$_2$CH$_2$O); 2.24 (s, 6H, 2 × CH_3); 2.45 (s, 6H, 2 × CH_3); 3.97 (t, J = 6.1 Hz, 4H, 2 × CH_2O); 3.99 (t, J = 6.5 Hz, 4H, 2 × CH_2O); 6.73 (s, 2H, arom); 7.05 (s, 2H, arom); 7.09 (d, J = 16.2 Hz, 2H, H_{vinyl}); 7.13 (d, J = 15.8 Hz, 2H, H_{vinyl}); 7.17 (d, J = 15.8 Hz, 2H, H_{vinyl}); 7.25 (d, J = 15.8 Hz, 2H, H_{vinyl}); 7.34 (d, J = 8.1 Hz, 4H, arom); 7.51 (d, J = 16.2 Hz, 2H, H_{vinyl}); 7.53 (d, J = 15.8 Hz, 2H, H_{vinyl}); 7.56 (s, 8H, arom); 7.59 (s, 8H, arom); 7.50−7.60 (m, 4H, H_{vinyl}); 7.67 (d, J = 8.4 Hz, 4H, arom); 7.84 (s, 2H, arom (core)); 8.04 (d, J = 8.1 Hz, 4H, arom); 8.12 (d, J = 8.4 Hz, 4H, arom). IR (cm^{-1}): 3044 (m), 3033 (m), 2950 (s), 2922 (s), 2870 (s), 2852 (s), 1606 (s), 1594 (s), 1574 (m), 1554 (m), 1512 (s), 1493 (s), 1466 (s), 1454 (m), 1411 (s), 1390 (s), 1377 (m), 1310 (w), 1289 (w), 1272 (w), 1246 (w), 1205 (s), 1180 (s), 1117 (w), 1099 (w), 1066 (s), 1042 (m), 1034 (m), 1015 (m), 957 (s), 850 (s), 827 (s), 801 (s), 742 (m), 725 (s), 700 (m), 544 (m), 535 (s), 500 (m). MS (MALDI): *m*/*z* 1750.98 (M$^+$ (calcd: 1751.03)).

(*Z*)-2-(4-(*E*)-2-[4-Methyl-2,5-bis(octyloxy)phenyl]ethenylphenyl)-3-(4-(*E*)-2-[2,4,5-tris((*E*)-2-4-[(*Z*)-2-(4-(*E*)-2-[4-methyl-2,5-bis(octyloxy)phenyl]ethenylphenyl)-3-nitrilo-1-propenyl]-phenyl ethenyl)phenyl]ethenylphenyl)-2-propenenitrile, CN-X. The following procedure was adapted from the literature.[20] The mixture of 4-((*E*)-2-{2,4,5-tris[(*E*)-2-(4-formylphenyl)-ethenyl]phenyl}ethenyl) benzencarbaldehyde,[13] **8**, (150 mg, 0.25 mmol) and 2-(4-(*E*)-2-[4-methyl-2,5-bis(octyloxy)phenyl]ethenylphenyl)acetonitrile, **9**, (730 mg, 1.5 mmol) was stirred in THF (15 mL) and *tert*-butyl alcohol (15 mL) for ~2 h to ensure complete dissolution. The reaction temperature was raised to 50 °C after which 0.05 mL of tetrabutylammoniumhydroxide was added, and the reaction continued for an additional 2 h. After cooling to room temperature the solution was further stirred for 8 more hours to complete the reaction. The resulting mixture then was precipitated from methanol, and the solid was collected by filtration and dried. The product was purified by column chromatography using a petroleum ether and ethyl acetate mixture (6:1) as an eluent to yield 320 mg (yield 51%) of pure (red) product. ^{1}H NMR (360 MHz, $CDCl_3$), δ (ppm): 0.78−0.94 (m, 24H, 8 × CH_3); 1.18−1.58 (m, 80H, 40 × CH_2); 1.70−1.92 (m, 16H, 8 × *CH*$_2$CH$_2$O); 2.24 (s, 12H, 4 × CH_3); 3.98 (t, J = 6.1 Hz, 16H, 8 × OCH_2); 6.74 (s, 4H, arom); 7.04 (s, 4H, arom); 7.09 (d, J = 16.6 Hz, 4H, H_{vinyl}); 7.19 (d, J = 15.8 Hz, 4H, H_{vinyl}); 7.54 (d, J = 16.6 Hz, 4H, H_{vinyl}); 7.56 (s, 4H, 4 × C═CHCN); 7.58 (d, J = 8.4 Hz, 8H, arom); 7.62 (d, J = 15.8 Hz, 4H, H_{vinyl}); 7.69 (d, J = 8.4 Hz, 8H, arom); 7.69 (d, J = 8.3 Hz, 8H, arom); 7.90 (s, 2H, arom (core)); 7.98 (d, J = 8.3 Hz, 8H, arom). IR (cm^{-1}): 3082 (w), 3058 (w), 3026 (m), 2950 (s), 2922 (s), 2868 (s), 2851 (s), 2212 (m), 1626 (w), 1599 (s), 1581 (m), 1513 (s), 1502 (s), 1466 (s), 1453 (s), 1410 (s), 1388 (m), 1377 (m), 1338 (m), 1308 (m), 1276 (w), 1261 (m), 1205 (s), 1188 (m), 1119 (m), 1064 (m), 1050 (m), 1030 (s), 962 (s), 953 (m), 945 (m), 892 (w), 849 (m), 815 (m), 806

(m), 765 (w), 746 (w), 721 (w), 696 (m), 538 (m), 511 (w). MS (MALDI): *m*/*z* 2483.86 (M^+ (calcd: 2483. 61)).

Thermal Analysis. Thermogravimetric analysis (TGA) was conducted on a Perkin-Elmer system with a TGA/7 thermogravimetric analyzer under a heating rate of 10 °C/min and a nitrogen flow. Differential scanning calorimetry was performed on a Perkin-Elmer DSC/7 differential scanning calorimeter. Samples were encapsulated in aluminum pans and were heated and cooled at a rate of 5 °C/min. Melting and crystallization points were determined by extrapolation to baseline from the slope of the onset of the transition.

X-ray Diffraction Analysis. Small-angle X-ray scattering (SAXS) and wide-angle X-ray scattering (WAXS) techniques were used to probe the samples for morphological order. SAXS data were collected at room temperature using a Rigaku Rotoflex rotating Cu anode source, operated at a 30 kV and 100 mA, an Anton-Paar HR PRK pinhole collimation X-ray camera, and a Brüker AXS Hi-Star 2-D area detector. The sample to detector distance was 23 cm. Samples approximately 2 mm thick and 5 mm in diameter were sandwiched between layers of Kapton tape. Data were corrected for background scattering, then azimuthally averaged for analysis as $I(q)$ as a function of q, where $q = 4\pi \sin(\theta)/\lambda$, θ is one-half the scattering angle 2θ, and λ is the X-ray wavelength, 1.54 Å. WAXS data were collected using a Siemens D5005 powder X-ray diffractometer, with a sealed X-ray tube source, operated at 40 kV and 40 mA. Powdered samples were placed on a low-background quartz sample holder and locked-coupled scanned from 30° to 90° 2θ. The one-dimensional data are shown as collected.

Electron Diffraction. Selected area electron diffraction patterns were recorded using a JEOL 2000 electron microscope operated at an accelerating voltage of 200 kV at a camera length of 120 cm. A drop of solution containing *p*-OXA-X in THF was placed on a carbon-coated commercial copper grid for electron microscopy (400 mesh). After slow evaporation of the liquid in a solvent-saturated atmosphere at room temperature, the grid was introduced in the electron microscope chamber.

Photophysical Characterization. UV−vis spectra were measured on a Beckman DU 640 and an Agilent 8453 spectrophotometer. Luminescence spectra were recorded on a SPEX Fluoromax 3 using DataMax software. Quantum efficiencies of the compounds in THF were measured relative to coumarin 314 in dilute ethanol solution according to the method of Williams et al.[21]

Device Fabrication and Testing. These were performed as described earlier.[22]

Results and Discussion

Synthesis/Characterization. For the synthesis of PPV-X, *o*-, and *p*-OXA-X (Scheme 1) we applied an orthogonal approach using an alternation of the Horner−Emmons and Heck reactions. It consisted of the separate preparation of the conjugated "arms" terminated by aldehyde and vinyl functionalities (**1**, **2**, **3**), and the preparation of a core, containing phosphonate-activated methylene and bromine groups (**4, 6**). The next step was the double Horner−Emmons reaction of two molar equivalents of **1** and one equivalent of 2,5-bis(diethylphosphonatomethyl)-1,4-dibromobenzene,[13] **4**. The resulting linear precursor **5** was further used in a Heck reaction with two molar equivalents of another vinyl-terminated intermediate **2** to give PPV-X (Scheme 1) in good yield. The reaction of **5** with oxadiazole-incorporated intermediate **3** resulted in *p*-OXA-X. Use of 4,5-dibromo-2-[(diethoxyphosphoryl)methyl] benzylphosphonate,[16,17] **6**, as a core led to the synthesis of the oligomer with conjugated arms, containing oxadiazole rings, in ortho position to each other, *o*-OXA-X. To synthesize the cyano molecule (CN-X) a different approach was used. Acetonitrile-terminated arm **9** was synthesized from 2-(4-vinylphenyl)acetonitrile[18] and 1-iodo-2,5-bis-(octyloxy)-4-methylbenzene by a Heck coupling reaction. Subsequently, a Knoevenagel condensation[20] of 4-(2-{2,4,5-tris-[2-(4-formylphenyl)ethenyl]phenyl}ethenyl)benzencarbaldehyde,[13] **8**, with a 6-fold excess of **9** gave CN-X in good yield (51%). All reactions yielded selectively only trans isomers. As can be seen from Chart 1 and Scheme 1, these synthetic approaches are very versatile for the preparation of different X structures. Once a collection of vinyl- and aldehyde-terminated arms are prepared, they can be used with different bifunctional cores to prepare a variety of molecules whose structure vary in arm composition, placement, and length.

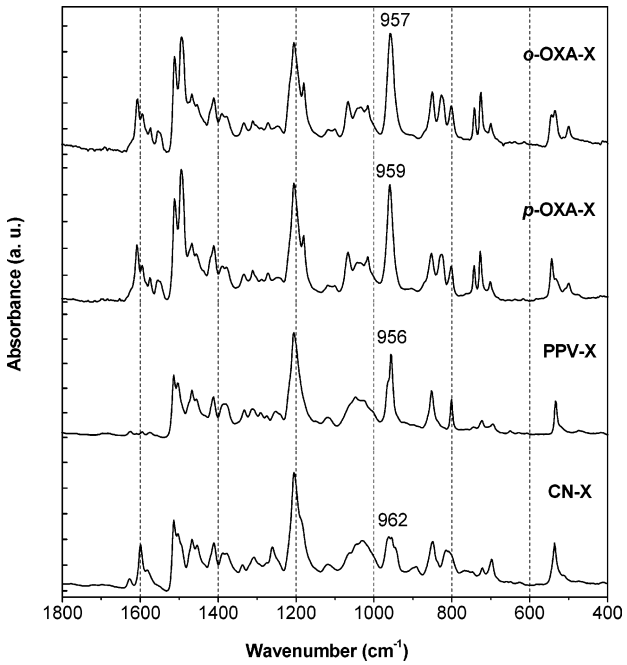

Figure 1. IR spectra of *o*-OXA-X, *p*-OXA-X, PPV-X, and CN-X in KBr pellets.

The structures of all oligomers were analyzed and confirmed by ^{1}H NMR, MS, and FT-IR analyses. The observed coupling constant values for the vinyl protons are in the region of ^3J = 15.8−16.4 Hz which is consistent with an all-trans configuration[23] for all compounds. Signals from aromatic and vinyl protons for *p*-, *o*-OXA-X, and CN-X in the aromatic region were difficult to assign due to overlapping of the vinyl and phenyl protons. Therefore a 2-D NMR COSY experiment was applied. Based on coupling constants and the COSY experimental data, we were able to assign most of the peaks. However two H_{vinyl} signals for the *o*-OXA-X in the region of 7.5−7.6 ppm remained unresolved (see the Supporting Information).

The all-trans configuration was also confirmed by IR (Figure 1) where the *trans*-vinylene HC═CH out-of-plane bending deformation band for all oligomers was observed at 956−962 cm^{-1} in accordance with literature data.[24] The IR strong absorption band at 1205 cm^{-1} appeared for all oligomers due to the antisymmetric C−O−C vibrational mode, whereas symmetric C−O−C stretch occurred in the 1015 to 1066 cm^{-1} region. The IR spectrum of CN-X exhibited a band at 2212 cm^{-1}, which is a characteristic of C≡N group.

IR spectra for the para- and ortho-substituted Xs were very similar except for the intensities of peaks at 543 and 532 cm^{-1}, which are due to skeletal deformation. The C═C absorption

SCHEME 1: Synthetic Scheme of PPV-X, *p*- and *o*-OXA-X, and CN-X

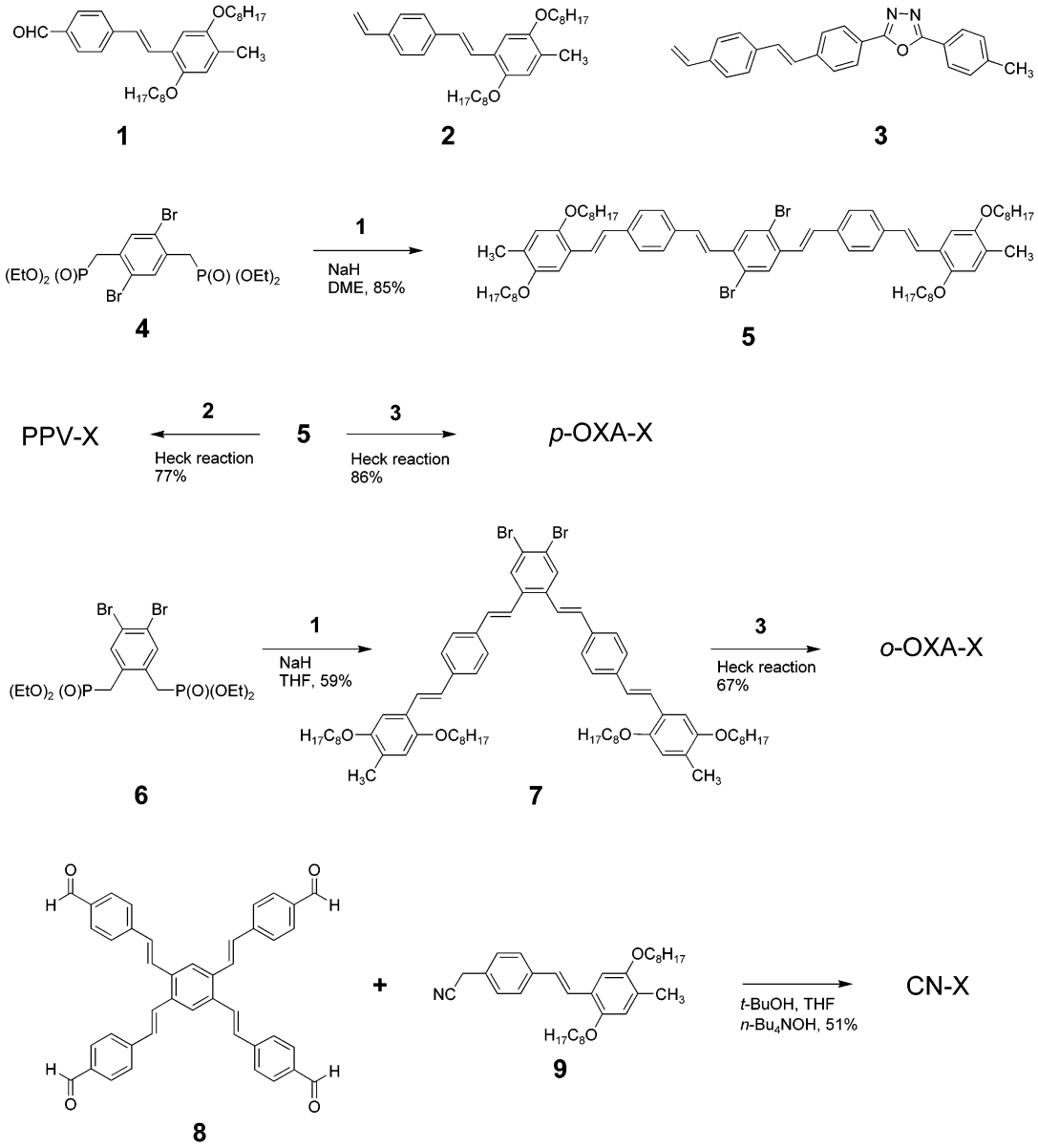

bands in the region of 1625−1580 cm^{-1} are almost absent in the PPV-X spectrum, which could be attributed to its 4-fold symmetry.[23,24] However, the peaks appear in CN-X, although it is also symmetrical, owing to the presence of the C≡N group in conjugation with C═C.[23,24] In this same region the para and ortho OXA-Xs' IR spectra exhibit a C═N stretching mode. The MALDI mass spectra of all Xs showed the molecular ion peak at the calculated position.

Physical Properties. Thermogravimetric analysis and differential scanning calorimetry were used to investigate the melting points and thermal stability of all the X molecules. The results are summarized in Table 1. None of the 2-D oligomers show any significant (∼2%) weight loss under heating in nitrogen to a temperature of 350 °C and exhibit an onset for degradation at ∼400 °C. The maximum rate of weight loss takes place at ∼430 °C for PPV-X and *o*-OXA-X, whereas for CN-X and *p*-OXA-X it is seen at 438 °C and 445 °C, respectively. Above 600 °C about 25 wt % residue of PPV-X was formed while ∼33 wt % and ∼35 wt % residues were observed for cyano- and oxadiazole-containing oligomers, respectively.

The DSC results indicate that the oxadiazole molecules, particularly the *p*-OXA-X, have a higher melting point than CN-X, which in turn has a higher melting point than the PPV-X (Table 1). This is consistent with having eight long amorphous alkoxy groups in PPV-X compared to only four in OXA-Xs. Additionally, incorporation of the more polar oxadiazole ring and cyano group would increase the intermolecular interaction. Since devices such as LEDs heat during operation, the high melting points of the CN-X and the oxadiazole Xs bode well for their use. All the molecules except CN-X crystallize during the cooling cycle. The *o*-OXA-X differs from the other molecules in that it consistently showed two melting and

TABLE 1: Thermal Properties of the X Molecules as Measured by DSC and TGA[a]

compound	T_m (°C)	T_c (°C)	T_d (°C)
PPV-X	119	88	428
p-OXA-X	240	198	445
o-OXA-X	195, 227[b]	163, 196	430
CN-X	154		438

[a] Transition temperatures (T_m and T_c) for the first heating and cooling cycles (5 °C/min). [b] Melting peaks are given for the second heating cycle (5 °C/min). In the first heating cycle a broad unresolved transition from 190 to 225 °C was observed.

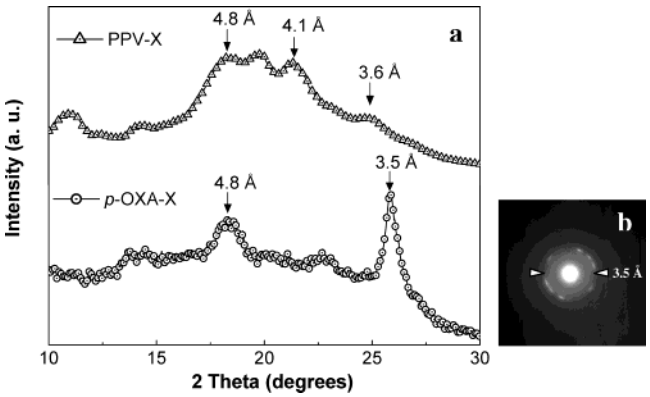

Figure 2. (a) Wide-angle X-ray diffraction data of powder PPV-X (△) and *p*-OXA-X (○). (b) Selected area electron diffraction pattern for *p*-OXA-X film from THF solution by drop-cast.

crystallization peaks. Both were completely reversible and reproducible through repeated scanning. Further study is needed to explain these data; however, it is important to note that the molecules were designed to $\pi-\pi$ stack and could be expected to form discotic liquid crystals explaining the presence of two transitions.

X-ray Diffraction Data. To better understand the morphological behavior of these molecules, preliminary wide-angle and small-angle X-ray scattering experiments were performed on powdered samples of PPV-X and *p*-OXA-X. Both materials show evidence of a large degree of ordering on both short and long length scales. The WAXS data are shown in Figure 2a. Evidence of strong $\pi-\pi$ stacking, usually indicated by a peak near 3.5 Å,[6,12,25] is observed for *p*-OXA-X. In addition to the 3.5 Å peak, there is a strong reflection corresponding to *d* spacing of 4.8 Å, which may be related to the length of the *a*-axis as observed in the triclinic single-crystal structure of phenylenevinylene-based linear molecules.[6,26] In PPV-X a weak peak at 3.6 Å and stronger reflections at 4.1 Å and above are observed. The 3.6 Å reflection in PPV-X is, however, much weaker than the 3.5 Å reflection in p-OXA-X. These data indicate that $\pi-\pi$ stacking, if present in PPV-X, is much weaker than in *p*-OXA-X.

Since the diffraction studies were done on powders and the molecules are used in films spun from solution, we decided to investigate the morphology that exists in films using electron diffraction and NMR. Electron diffraction of *p*-OXA-X was done on a film drop-cast from THF and is shown in Figure 2b. The outer ring in the diffraction pattern corresponds to the spacing of 3.5 Å and confirms the propensity of these molecules to $\pi-\pi$ stack.

The strong tendency of the *p*-OXA-X to $\pi-\pi$ stack is also observed in NMR experiments done in solution. The chemical shifts of the oxadiazole oligomer *p*-OXA-X are dependent on concentration (Figure 3). The signals from aromatic and vinylene protons are shifted upfield in concentrated $CDCl_3$ solution due to intermolecular interaction.[27] For instance, the singlet peak from core protons shifted from $\delta = 7.86$ to $\delta = 7.73$ ($\Delta\delta = 0.13$). The signal of the protons on the outer benzene ring of the PPV arms of *p*-OXA-X with octyloxy substituents hardly shifted with concentration ($\Delta\delta \approx 0.02$). This may be explained if the planar conformation for the central part of *p*-OXA-X results in self-association in solution through $\pi-\pi$ interactions yielding columnar stacks of liquid crystals.[27,28] Interestingly, *o*-OXA-X and CN-X also exhibit the same shift in NMR peak position with concentration, supporting the hypothesis that these molecules assemble in concentrated solutions. This is significant since researchers have shown[29,30] that the conformation and aggregation that exists in solution is transferred onto films spun from these solutions. Thus, these molecules in films used in devices such as LEDs should have some $\pi-\pi$ interactions. Consistent with the X-ray results, the PPV-X does not exhibit any significant shift in NMR peaks with concentration, indicating that $\pi-\pi$ interactions, if they exist in PPV-X films, are much weaker than in films of the other X molecules. Further work will be done to quantify and better understand the extent to which the molecules associate in the films used in devices.

Photophysical Properties. The photophysical properties of these molecules can in part be understood by contrasting their behavior to linear analogues. To accomplish this, we used a pentamer of PPV and a polymeric PPV (with $M_n = 4200$), whose properties have been reported previously,[22] as models for PPV-X. The pentamer was chosen because one branch of the PPV-X (two para arms on the central ring) is identical in composition to the PPV pentamer. The normalized absorption and emission spectra for these three materials in dilute THF solution and in films spun from TCE are presented in Figure 4.

The absorption maxima and band edge of PPV-X in solution and film are blue-shifted and the vibronic features are less prominent as compared to that of PPV and the pentamer. As expected, the absorption in film is red-shifted compared to that

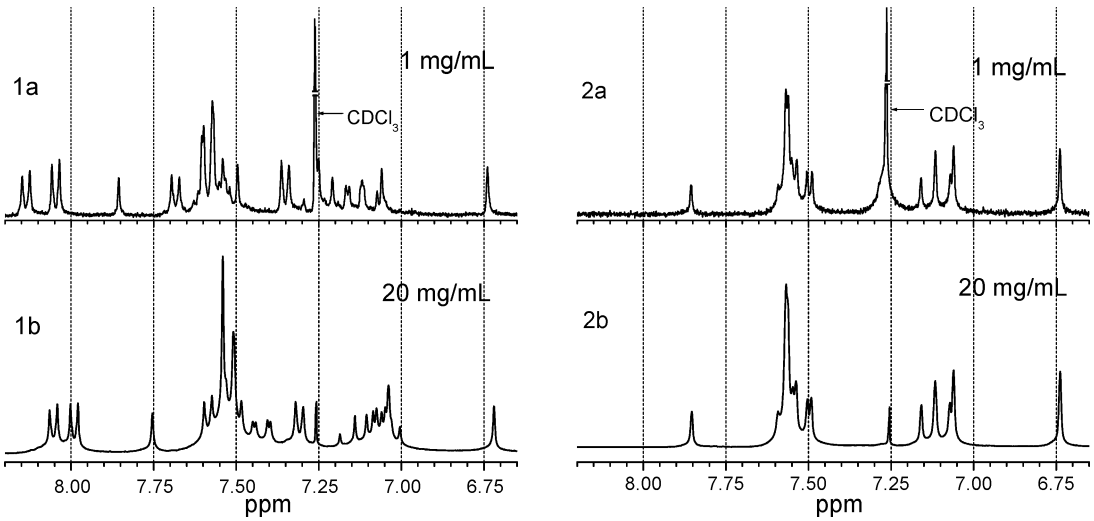

Figure 3. ^{1}H NMR spectra (360 MHz, room temperature) of *p*-OXA-X (1a, b) and PPV-X (2a, b) in $CDCl_3$ at different concentrations: (1a, 2a) 1 mg/mL and (1b, 2b) 20 mg/mL (the same concentration used for device fabrication).

TABLE 2: Photophysical Properties of X Molecules

	absorption			emission				
compound	solution λ_{max} nm	film λ_{max} nm	Δ_{soln} nm	solution λ_{max} nm	film λ_{max} nm	Δ_{film} nm	stokes shift eV	quantum yield in THF %
PPV	450	477	27	514	539	25	0.30	81
pentamer	430	431	1	483	524	41	0.51	63
PPV-X	395	417	22	476	542	66	0.68	77
p-OXA-X	389	416	27	497	547	50	0.72	56
o-OXA-X	400	412	12	485	550	65	0.76	65
CN-X	426	430	14	516	565, 605	49, 89	0.69	42

in solution as a result of an increase in the effective conjugation length which is caused by the chain backbone becoming more planar in the solid state.[31,32]

The emission maximum of PPV-X in solution is blue-shifted compared to that of PPV but is similar to that of pentamer. The very close similarity of the PPV-X and pentamer emission in solution suggests that the molecule is very twisted in solution and emission is coming from one branch of the X. This changes significantly when comparing emission from the films. PPV-X has a red-shifted emission compared to that of the pentamer, and its peak maximum is close to that of PPV, but the emission spectrum is featureless and broader than that of PPV. As we show later, this broad emission from a film and large Stokes shift, 0.68 eV for PPV-X, is common to all the X molecules.

There are two contributing factors that may explain the Stokes shift and the breadth of the emission. A large Stokes shift is observed when the geometry between the ground and excited state is very different. If the charge is delocalized over the entire X molecule in the excited state, then the geometry change would be larger than in linear molecules. A second contributing factor to the large Stokes shift and broad emission could be excimer formation since in organic solids this is exhibited as broad, featureless and red-shifted emission. Molecules with strong intermolecular interactions leading to cofacial chain packing in the solid state and also having interplanar distances of 3.3−3.6 Å tend to form excimers.[31−39] PPV-X has potential for $\pi-\pi$ stacking although the X-ray of crystals did not have a prominent peak around 3.5 Å. The NMR studies did not indicate any $\pi-\pi$ stacking in concentrated solutions, perhaps because of the presence of alkoxy groups on all four arms. It is important to remember, however, that neither of these is a direct measure of morphology in the films used for photoluminescence or LEDs. The morphology could be different and excimers may still form in the PPV-X films. The contribution of excimers to photoluminescence will be further investigated in the future using time-resolved and temperature-dependent photoluminescence studies.

The results of a preliminary investigation of the photophysical properties of all the X molecules are shown in Table 2 and Figure 5. The UV−vis absorption spectra are red-shifted in films spin-coated from TCE as compared to those in dilute THF solution, and concomitant with this bathochromic shift the absorption peaks in film have acquired shoulders not present in solution. The absorption spectra of CN-X in solution and film are red-shifted compared to those of PPV-X, *p*-OXA-X, and *o*-OXA-X as is expected from a previous report on linear cyano-PPV compared to PPV.[20] The absorption spectra of PPV-X, *p*-OXA-X, and *o*-OXA-X in film show similar features and peak maxima also consistent with studies on linear polymers that showed that incorporation of oxadiazole into PPV did not shift absorption peaks.[14] In solution the absorption spectra of *o*-OXA-X and PPV-X are almost identical, whereas the spectrum of *p*-OXA-X is broader and the maximum peak is slightly blue-shifted, even though the absorption edge is the same as in *o*-OXA-X and PPV-X.

As seen with PPV-X, the emission spectra of *o*-OXA-X and CN-X in dilute THF solution show varyingly strong vibronic features. The emission spectrum of *p*-OXA-X is, however, broad and featureless in solution. It can also be observed that the substitution of oxadiazole groups in the ortho position makes no significant difference in the absorption and emission spectra in solution or film as compared to that of PPV-X. The emission maxima of CN-X in solution and film are highly red-shifted compared to those of other compounds. The S_0-S_0 transition in film emission for CN-X is seen as a small shoulder and is at a lower intensity compared to the S_0-S_1 transition. There is also a hint of the shoulder in the PL spectra from films of *p*-OXA-X and *o*-OXA-X. The red-shift for CN-X may be

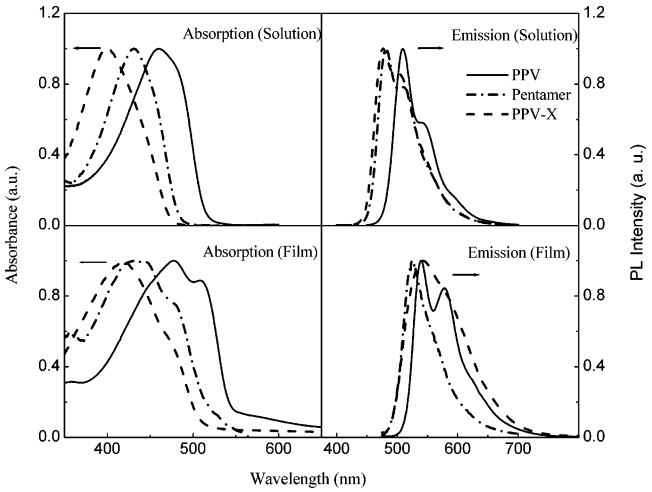

Figure 4. Normalized absorption and emission spectra of PPV (solid line) and pentamer (dash dot) in comparison with PPV-X (dash) in dilute THF solution and film spin-coated from TCE.

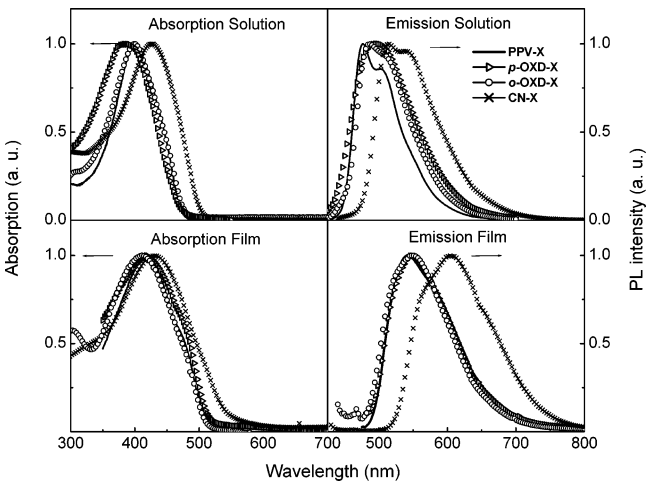

Figure 5. Normalized absorption and emission spectra of PPV-X (solid line), p-OXA-X (△), o-OXA-X (○), and CN-X (×) in dilute THF solution and film spin-coated from TCE.

TABLE 3: Device Efficiency Data of Investigated Oligomers PPV-X, *o*-OXA-X, *p*-OXA-X, CN-X, and PPV

material	Ext. EL efficiency %	Turn On Voltage V
Single-Layer Device		
PPV	0.011	9
PPV-X	0.003	6
o-OXA-X	0.015	11
p-OXA-X	0.021	6
CN-X	0.002	12
50% PPV:50% PPV-X	0.032	7
50% PPV:50% *p*-OXA-X	0.044	7
Multilayer Device[a]		
p-OXA-X	0.20	4
CN-X[b]	0.10	7

[a] Device configuration Glass/ITO/PEDOT:PSS(120 nm)/EL(120 nm)/LiF(~0.7 nm)/Al(200 nm). [b] Toluene was used as solvent.

attributed to the presence of strong electron-withdrawing cyano groups and longer conjugation length.[40]

As noted earlier, the emission spectra of all the X molecules in films spin-coated from TCE are highly red-shifted, broader, and with a featureless vibronic structure as compared to that in dilute THF solution. The compounds also exhibit a large Stokes shift in the range of 0.6−0.8 eV as presented in Table 2. These characteristics are similar to those observed for PPV-X. Such shifts could suggest excited state delocalization in more than one dimension, aggregation, $\pi-\pi$ overlap, and/or interchain excimer formation.[31−39] The $\pi-\pi$ stacking in *p*-OXA-X, as confirmed by X-ray diffraction and NMR studies, lies within the range of an attractive excimer interaction. In ^{1}H NMR spectra phenyl and vinyl protons signals shift with increasing concentration, as seen for *p*-OXA-X (Figure 3), *o*-OXA-X, and CN-X, indicating that $\pi-\pi$ interactions exist in these solutions and thus are likely to exist in the films. If the large Stokes shift were due entirely to excimer formation that occurs because of strong $\pi-\pi$ interactions, we would expect to see a difference in the Stokes shift for films of PPV-X where the NMR data indicate that no $\pi-\pi$ interactions exist. It is, therefore, possible that delocalization of the charge in the excited state over all four arms increases the geometry change between the ground and excited states resulting in a large Stokes shift. The oligomers also exhibit very high quantum yields of 0.40−0.80 in solution. Despite the tendency of the OXA-Xs to $\pi-\pi$ stack, films of these compounds appear very fluorescent. We have not measured photoluminescent (PL) quantum yields of the films, but from PL intensity for films with similar absorbance, PPV-X and CN-X are slightly less fluorescent than PPV, while *o*- and *p*-OXA-X have similar fluorescence to a film of PPV. The $\pi-\pi$ stacking enabling 2-D or possibly 3-D delocalization of charge, a large Stokes shift, and high quantum yields make these compounds suitable candidates for application in electroactive devices.

Light-Emitting Diodes. Single-layer light-emitting diodes were fabricated by spin-coating a solution of the oligomers in TCE onto an indium tin oxide (ITO) substrate. Aluminum was evaporated on top of the active layer, and the device performance was recorded in an inert atmosphere. Table 3 provides efficiencies for these devices. LEDs prepared from the oxadiazole molecules performed better than those prepared from PPV-X. The *p*-OXA-X was particularly good despite the tendency of this oligomer to crystallize. When *p*-OXA-X was blended with PPV, the efficiency was very promising, indicating that hole transport in *p*-OXA-X may be limiting the device performance. It is important to note that none of the devices have been optimized.

Studies of multilayer devices with a hole-transporting layer, such as polyethylenethioxythiophene:poly styrene sulfonic acid (PEDOT:PSS) and LiF between the emissive and Al layers, has begun on some of the materials. As shown in Table 3, the external efficiency of these multilayer devices made from *p*-OXA-X and CN-X as the emissive layers increased from 0.021 and 0.002% to 0.20 and 0.10%, respectively. In the case of CN-X, which is an electron transporter, the dramatic improvement in device performance for the multilayer device is probably due to better charge balance. Since the *p*-OXA-X is better balanced in regard to hole and electron transport, the improvement in this device when going from the single layer to the multilayer configuration is more indicative of what can be expected from the other compounds. While this 10-fold increase is significant, device efficiencies can be further improved with changes in processing conditions such as solvent system, spin rate, electrodes, and annealing to alter film morphology.

Conclusion

A synthetic strategy has been developed that allows for the synthesis of a novel group of electroactive molecules with four conjugated arms extending from a central phenyl core. By varying the placement and composition of these arms, the properties of the molecules can be controlled. The molecule with four PPV arms, PPV-X, showed no indication of strong $\pi-\pi$ stacking while the oxadiazole and cyano-containing molecules all have some degree of $\pi-\pi$ interactions. All four molecules are thermally stable and solution-processible. The photoluminescent quantum yield in solution is good for all the molecules, which also have a large Stokes shift in comparison to their linear counterparts. This large Stokes shift, even in PPV-X where weak if any $\pi-\pi$ stacking is evident, suggests that delocalization of the charge in the excited state may be occurring over all the arms, although a more detailed study is needed to confirm this. Preliminary device data suggests that in spite of possible $\pi-\pi$ stacking in films, these molecules perform well in LEDs. Further studies on carrier mobility in the oxadiazole and cyano molecules is planned since the strong intermolecular interactions in these molecules should enhance mobility and make them useful in thin film transistors or photovoltaic devices.

Acknowledgment. The authors gratefully acknowledge the National Science Foundation for supporting this research under DMR Grants 9972880, 0208786 and for instrumentation funding under DMR Grant IMR-0196040. Partial funding was also provided by the DoD Materials Center of Excellence through the Center for Composite Materials at the University of Delaware. The authors are very grateful to Dr. Anoop Menon for the synthesis and photophysical data of the pentamer and PPV and to Mary Kurian, Dr. Chaoying Ni, and John Papalia for the X-ray and TEM data and to Professor Douglas J. Buttrey for helpful discussions on the TEM data.

Supporting Information Available: Experimental details of synthesis and characterization data for all compounds other than Xs, ^{1}H NMR, FT-IR, and 2-D NMR spectrum for *o*-OXA-X. This material is available free of charge via the Internet at http://pubs.acs.org.

References and Notes

(1) Friend, R. H.; Gymer, R. W.; Holmes, A. B.; Burroughes, J. H.; Marks, R. N.; Taliani, C.; Bradley, D. D. C.; Dos Santos, D. A.; Bredas, J. L.; Logdlund, M.; Salaneck, W. R. *Nature* **1999**, *397*, 121.

(2) Bernius, M. T.; Inbasekaran, M.; O'Brien, J.; Wu, W. S. *Adv. Mater.* **2000**, *12*, 1737.
(3) Wallace, G. G.; Dastoor, P. C.; Officer, D. L.; Too, C. O. *Chem. Innovation* **2000**, *30*, 14.
(4) Brabec, C. J.; Sariciftci, N. S.; Hummelen, J. C. *Adv. Funct. Mater.* **2001**, *11*, 15.
(5) Brown, A. R.; Bradley, D. D. C.; Burroughes, J. H.; Friend, R. H.; Greenham, N. C.; Burn, P. L.; Holmes, A. B.; Kraft, A. *Appl. Phys. Lett.* **1992**, *61*, 2793.
(6) Koren, A. B.; Curtis, M. D.; Kampf, J. W. *Chem. Mater.* **2000**, *12*, 1519.
(7) Sirringhaus, H.; Brown, P. J.; Friend, R. H.; Nielsen, M. M.; Bechgaard, K.; Langeveld-Voss, B. M. W.; Spiering, A. J. H.; Janssen, R. A. J.; Meijer, E. W.; Herwig, P.; de Leeuw, D. M. *Nature* **1999**, *401*, 685.
(8) Jakubiak, R.; Collison, C. J.; Wan, W. C.; Rothberg, L. J.; Hsieh, B. R. *J. Phys. Chem. A* **1999**, *103*, 2394.
(9) Son, S.; Dodabalapur, A.; Lovinger, A. J.; Galvin, M. E. *Science* **1995**, *269*, 376.
(10) Deb, S. K.; Maddux, T. M.; Yu, L. *J. Am. Chem. Soc.* **1997**, *119*, 9079.
(11) Robinson, M. R.; Wang, S. J.; Heeger, A. J.; Bazan, G. C. *Adv. Funct. Mater.* **2001**, *11*, 413.
(12) Schmidt-Mende, L.; Fechtenkotter, A.; Mullen, K.; Moons, E.; Friend, R. H.; MacKenzie, J. D. *Science* **2001**, *293*, 1119.
(13) Niazimbetova, Z. I.; Menon, A.; Galvin, M. E.; Evans, D. H. *J. Electroanal. Chem.* **2002**, *529*, 43.
(14) Peng, Z. H.; Bao, Z. N.; Galvin, M. E. *Adv. Mater.* **1998**, *10*, 680.
(15) Peng, Z. H.; Galvin, M. E. *Chem. Mater.* **1998**, *10*, 1785.
(16) Rivera, J. M.; Martin, T.; Rebek, J. *J. Am. Chem. Soc.* **2001**, *123*, 5213.
(17) Kimura, M.; Narikawa, H.; Ohta, K.; Hanabusa, K.; Shirai, H.; Kobayashi, N. *Chem. Mater.* **2002**, *14*, 2711.
(18) Wright, S. W.; McClure, L. D. *Org. Prep. Proced. Int.* **1994**, *26*, 602.
(19) Strey, B. T. *J. Polym. Sci., Part A: Polym. Chem.* **1965**, *3*, 265.
(20) Greenham, N. C.; Moratti, S. C.; Bradley, D. D. C.; Friend, R. H.; Holmes, A. B. *Nature* **1993**, *365*, 628.
(21) Williams, A. T. R.; Winfield, S. A.; Miller, J. N. *Analyst* **1983**, *108*, 1067.
(22) Menon, A.; Dong, H. P.; Niazimbetova, Z. I.; Rothberg, L. J.; Galvin, M. E. *Chem. Mater.* **2002**, *14*, 3668.
(23) Gordon, A. J.; Ford, R. A. *The Chemist's Companion. A Handbook of Practical Data, Techniques, and References*; Wiley: New York, 1972.
(24) Lin-Vien, D.; Colthup, N. B.; Fateley, W. G.; Grassetti, J. G. *The Handbook of Infrared and Raman Characteristic Frequencies of Organic Molecules*; Academic Press: Boston, 1991.
(25) Percec, V.; Glodde, M.; Bera, T. K.; Miura, Y.; Shiyanovskaya, I.; Singer, K. D.; Balagurusamy, V. S. K.; Heiney, P. A.; Schnell, I.; Rapp, A.; Spiess, H. W.; Hudson, S. D.; Duan, H. *Nature* **2002**, *419*, 384.
(26) van Hutten, P. F.; Krasnikov, V.; Brouwer, H. J.; Hadziioannou, G. *Chem. Phys.* **1999**, *241*, 139.
(27) Kraft, A. *Liebigs Ann/Recl.* **1997**, 1463.
(28) Palmans, A. R. A.; Vekemans, J.; Fischer, H.; Hikmet, R. A.; Meijer, E. W. *Chem.—Eur. J.* **1997**, *3*, 300.
(29) Collison, C. J.; Rothberg, L. J.; Treemaneekarn, V.; Li, Y. *Macromolecules* **2001**, *34*, 2346.
(30) Nguyen, T.-Q.; Martini, I. B.; Liu, J.; Schwartz, B. J. *J. Phys. Chem. B* **2000**, *104*, 237.
(31) Pope, M.; Swenberg, C. E. *Electronic Processes in Organic Crystals and Polymers*, 2nd ed.; Oxford University Press: New York, 1999.
(32) Birks, J. B. *Photophysics of Aromatic Molecules*; Wiley Monographs in Chemical Physics; Wiley-Interscience: London, New York, 1970.
(33) Samuel, I. D. W.; Rumbles, G.; Collison, C. J.; Moratti, S. C.; Holmes, A. B. *Chem. Phys.* **1998**, *227*, 75.
(34) Samuel, I. D. W.; Rumbles, G.; Collison, C. J.; Friend, R. H.; Moratti, S. C.; Holmes, A. B. *Synth. Met.* **1997**, *84*, 497.
(35) Samuel, I. D. W.; Rumbles, G.; Collison, C. J. *Phys. Rev. B: Condens. Matter* **1995**, *52*, 11573.
(36) Jenekhe, S. A.; Osaheni, J. A. *Science* **1994**, *265*, 765.
(37) Bredas, J. L.; Cornil, J.; Heeger, A. J. *Adv. Mater.* **1996**, *8*, 447.
(38) Nguyen, T.-Q.; Doan, V.; Schwartz, B. J. *J. Chem. Phys.* **1999**, *110*, 4068.
(39) Niazimbetova, Z. I.; Menon, A.; Galvin, M. E. *Polym. Prepr. (Am. Chem. Soc., Div. Polym. Chem.)* **2003**, *44*, 659.
(40) Sun, Y. M.; Hung, A. Y. C.; Wang, C. T. *J. Appl. Polym. Sci.* **2002**, *85*, 2367.